Monthly Notices of the ROYAL ASTRONOMICAL SOCIETY
MNRAS **455,** 3597–3611 (2016) doi:10.1093/mnras/stv2389

Super-Chandrasekhar dynamical friction in a constant-density spherical star system

M. I. Zelnikov[1,2★] and D. S. Kuskov[2,1★]
[1] *P. N. Lebedev Physical Institute of the Russian Academy of Sciences, Moscow 119991, Russia*
[2] *Moscow Institute of Physics and Technology, Dolgoprudny 141700, Russia*

Accepted 2015 October 13. Received 2015 October 6; in original form 2015 July 9

ABSTRACT

N-body modelling of massive body motion in constant density-cores shows deviations in the dynamical friction force from Chandrasekhar's formula. When the body orbit falls within the core, the body experiences a stage of enhanced friction after which the friction force becomes very low or zero. This effect takes place for circular as well as radial and elliptic orbits of the massive perturber. Previously developed perturbative treatment of dynamical friction in spherical systems cannot be directly applied to constant density cores because of the importance of non-linear resonant effects in this case. This feature is caused by the full resonance of the moving body with all the stars in the harmonic potential. There has been a successful attempt at semi-analytical treatment of the problem, but there remains a lack of any analytical description of this phenomenon. We study the motion of a massive point-like object in a strictly constant density sphere analytically and obtain a formula for the energy decay rate of the object at the stage of super-Chandrasekhar friction. We show that the dynamical friction force at this stage is half an order in $M_{\rm object}/M_{\rm core}$ stronger than in Chandrasekhar's case. Our numerical simulations for both circular and radial orbits of the perturber reveal the stage of enhanced friction and the stalling stage afterwards. Dependence of the decay time at the super-Chandrasekhar stage on the perturber mass confirms our analytical relationship. We compare our analytical formula with *N*-body results of other authors for the enhanced friction stage and find good agreement.

Key words: galaxies: formation – galaxies: haloes.

1 INTRODUCTION

In his pioneering paper, Chandrasekhar (1943) showed that a heavy body of mass M moving through an infinite homogeneous and isotropic medium of non-colliding lighter particles suffers a drag force. The body deflects trajectories of the background particles (BPs) by its gravitational field, and its total momentum loss due to this interaction is given by the formula

$$M\frac{\mathrm{d}V}{\mathrm{d}t} = -\frac{4\pi\, G^2\, M^2}{V^2}\ln\Lambda\rho(<V), \qquad (1)$$

where V is the speed of the object, $\rho(<V)$ is the density of particles with speeds less than V, and $\Lambda = p_{\max}/p_{\min}$. The quantities $p_{\max}$ and $p_{\min}$ are the maximum and minimum impact parameters of the encounters contributing to the drag, respectively. In general $p_{\max} \approx D$, where D is the size of the system and $p_{\min} \approx \max\,(Gm/V^2, d)$, where d is the size of the object and m is the single particle mass (e.g. White 1976). Generally, this force can also be understood as being caused by the gravitational attraction of a density wake, formed behind the moving body due to the perturbation of the medium by its own gravitational field (e.g. Mulder 1983).

Dynamical friction plays an important role in astrophysics. It influences the dynamics of galaxies in clusters, black holes (BHs) and globular clusters (GCs) motion, galactic bars rotation, etc. It governs satellite sinking and mass segregation processes in star clusters and galaxies, and all these phenomena have observational consequences.

Chandrasekhar's formula (1) turns out to work remarkably well in many cases (White 1983; Bontekoe & van Albada 1987; Zaritsky & White 1988; Cora, Muzzio & Vergne 1997), even beyond the approximation of the infinite, homogeneous, and isotropic medium used for its derivation. In particular, it is valid for the motion of a massive body in inhomogeneous systems with non-Maxwellian velocity distribution, after appropriate corrections of the Coulomb logarithm $\ln\Lambda$ and density expression to account for the density variation along the massive body trajectory and the influence of stars moving faster than the perturber (Colpi & Pallavicini 1998; Antonini & Merritt 2011). Corrected for velocity anisotropy, Chandrasekhar's formula can also be applied to aspherical systems (Peñarrubia, Just & Kroupa 2004).

★E-mail: zelnikov@lpi.ru (MIZ); dmitry.kuskov@phystech.edu (DSK)

However, it has been found that Chandrasekhar's formula loses its validity in constant-density cores. This is all the more interesting because observations of some galaxies showed that their central dark-matter cores are of almost constant density (de Blok et al. 2001; Borriello & Salucci 2001; Binney & Evans 2001; Kleyna et al. 2003).

Goerdt et al. (2006) found that, if a galaxy has a central constant-density core, then an orbiting satellite ceases sinking and stalls many dynamical times at the outer boundary of the core. So the dynamical friction in a constant density core tends to zero, in contradiction to the expectation of the Chandrasekhar's formula (1). Having investigated through *N*-body simulations the sinking of a massive perturber in cusped distributions with the slope γ not steeper than approximately 0.5, they also obtain the stalling behaviour of the satellite, caused by the transformation of the cusp into a constant density core due to the tidal influence of the sinking perturber. Only cusps steeper than $\gamma = 0.5$ survive, and in this case Chandrasekhar's formula is shown to describe the dynamical friction fairly well. So Goerdt et al. (2006) concluded that the dynamical friction force, while being well described by the Chandrasekhar formula for cuspy mass distributions, becomes zero in constant density cores. The authors believe that this effect is due to orbit-resonant scattering.

More insight into the physics of dynamical friction was provided by Read et al. (2006), who presented *N*-body and semi-analytical consideration of a satellite (GC) sinking into a spherical constant-density galactic core. The semi-analytical model assumes that the gravitational potential is purely harmonic, as it should be for strictly constant density spherical mass distribution. Read et al. (2006) neglected the back reaction of the mean gravitational field on the perturber and the BPs motion, so the gravitational potential was considered to be quadratic and fixed during all of the evolution. In this approximation, under the condition that the perturber orbit is fixed, and neglecting interactions between BPs themselves, the equation of motion of each BP can be written in a closed form (equation 10 in Read et al. 2006). The authors solved numerically this (non-linear) equation for each BP which allowed the traceing of the evolution of the density and velocity distribution of these particles. The authors stated that the results of these semi-analytical calculations confirm the results of their more accurate *N*-body simulations. The *N*-body model of Read et al. (2006) assumes the initial BP density distribution to have a plateau at the centre and power-law decay at large distances. The satellite orbit and gravitational potential are now live, evolving under the influence of BP motion. Read et al. (2006) found that sinking satellites experience an initial stage of very rapid (super-Chandrasekhar) dynamical friction, and a stage of very small or zero friction afterwards. This is shown to be true not only for circular satellite orbits, but for elliptical ones as well. Numerical data of Read et al. (2006) showed that the inspiralling satellite generally induces a rotating overdense region ('wake') of a scale comparable to the core size. The position of the centre of mass of the wake and relative phase of its rotation with respect to the satellite differ at the super-Chandrasekhar and stalling stages.

The essential statements of Read et al. (2006) about the physics of dynamical friction in constant density cores could be expressed as follows: (1) all BPs are in resonance with a massive satellite, if we neglect the back influence of the background perturbation to the satellite; (2) this resonant interaction results in the motion of BPs on stable epicycles about the perturber; (3) there is no time-averaged energy and momentum transfer between the satellite and BPs in equilibrium, and this is a reason for the very small friction of the satellite at the last stage; (4) when the satellite nears the constant-density core, a rearrangement of BP distribution from one equilibrium state to another results in the super-Chandrasekhar dynamical friction.

Goerdt et al. (2010) performed *N*-body modelling of a massive satellite sinking into cuspy backgrounds for a set of cusp slopes in the range $\gamma = 0.5$–1.75 and satellite masses from 10^5 to 5×10^7 solar masses. They found that the sinking satellite tidally transforms the cusp into a constant-density core and then stalls at the outer edge of this newly created core. Goerdt et al. (2010) showed that for circular and slightly eccentric orbits the satellite experiences a stage of enhanced friction, then after a small 'kickback' the satellite sinking stops. Goerdt et al. (2010) did not model a satellite sinking into a core that is of constant density from the very beginning. In their models, such cores are formed from a cuspy background only during the stage of enhanced friction. When the core formation is finished, the dynamical friction disappears. It should be noted that at the stage of zero friction the modelling shows satellite energy fluctuations near its mean value. This may be a result of the core-satellite system oscillations just after the core formation, or may be for other reasons. Goerdt et al. (2010) found that the mass of the core formed is of the order of the mass of the initial background, enclosed inside a tidal radius, so more massive satellites generates larger cores. The core is smaller as the initial cusp becomes steeper.

It is known that after supermassive BH binary merging the newly formed BH can obtain a significant recoil velocity due to an anisotropic emission of gravitational waves (Campanelli et al. 2007; Gonz'alez et al. 2007; Tichy & Marronetti 2007). Gualandris & Merritt (2008) have numerically analysed the motion of a supermassive BH kicked out of the centre of a galaxy core with $\rho \propto r^{-\gamma}$, $\gamma = 0.55$ initial density profile at the centre. It was shown (see section 4 of Gualandris & Merritt 2008) that such shallow cusp easily transforms by moving BH into almost constant-density core. If the kick velocity is large enough to remove the BH from the core, the BH starts radial oscillations with decreasing amplitude. The authors noted that in this case moving BH also generates a wake. However, in contrast to the case of the circular motion of the perturber discussed in Goerdt et al. (2006), Read et al. (2006), and Goerdt et al. (2010), the wake of a radially oscillating BH never has a chance to reach a steady-state form because the position and velocity of the BH change drastically during one crossing time. As one can conclude, the wake also oscillates and changes its form (see e.g. fig. 9 of Gualandris & Merritt 2008). For sufficiently large kick velocities, Gualandris & Merritt (2008) have found three stages of the BH motion: after a stage with Chandrasekhar friction (I) there follows a stage with very low (sub-Chandrasekhar) friction (II), and eventually the BH reaches thermal equilibrium with the stars (III). Numerical data of Gualandris & Merritt (2008, Figs 3 and 6 of this paper) reveal a prominent 'knee' in the energy dependence of the BH between stages I and II, which means a quick (super-Chandrasekhar) deceleration at the end of the first Chandrasekhar stage. However, they did not single out this period of enhanced friction and did not investigate it.

Analogous results for a constant-density core galaxy have been obtained by Read et al. (2006) and Inoue (2011). In their numerical calculations, they have shown that after a stage with super-Chandrasekhar friction there comes a stage with almost no friction.

Comparing *N*-body results of Gualandris & Merritt (2008), Goerdt et al. (2006), Read et al. (2006), and Goerdt et al. (2010), we see that, in constant-density cores, a massive perturber runs qualitatively through the same stages of motion – Chandrasekhar, super-Chandrasekhar, sub-Chandrasekhar – no matter whether its orbit is circular, elliptical, or radial. As we shall argue, this similarity is not fortuitous and reveals the common physics of dynamical friction in constant-density cores, whereas inhomogeneities, induced by circular and radially moving perturbers are apparently quite dissimilar.

There have been a number of attempts to understand the cause of non-Chandrasekhar dynamical friction and to generalize Chandrasekhar's formula to the case of constant density cores. Kalnajs (1972) has computed dynamical friction in a uniformly rotating disc of stars analytically and has demonstrated that owing to collective effects in this self-gravitating disc the dynamical friction in this system disappears. In order to get further insight into the physics of dynamical friction phenomena gravitationally bound mass distributions, Tremaine & Weinberg (1984) and Weinberg (1986) formulated a perturbative theory of dynamical friction in spherical systems. They considered the circular motion of a massive body in a galaxy with generic spherical potential. Tremaine & Weinberg (1984) have shown that dynamical friction, exerted on a body rotating in a spherical galaxy, is caused mostly by stars that are in resonance with the body, i.e. moving with the same (or a commensurable) period. As the rotational frequency of the body changes due to dynamical friction, the body gradually passes through resonances with different groups of stars. Tremaine & Weinberg (1984) discovered that the character of the star's response to the perturbation depends on a dimensionless parameter that has a sense of the speed of the transition through resonances. For a fast passage through resonances the dynamical friction is given by formula (93) in Tremaine & Weinberg (1984), which is an analogue of Lynden-Bell & Kalnajs (1972) formula and can be considered as a generalization of Chandrasekhar's formula for a spherical system. For slow resonance passage in a spherical star systems, the energy exchange between the perturber of mass M and a BP is shown to be reversible ('dynamical feedback') and $O(M^{1/2})$ stronger, than the Lynden-Bell and Kalnajs formula (which is analogous to and of the same order as Chandrasekhar's friction).

Following Tremaine & Weinberg (1984) and Weinberg (1986), most researchers recognize the clue role of resonant interaction for dynamical friction in spherical systems in general. However, there is no agreement so far about the cause of the enhanced friction and friction damping in constant-density cores. Read et al. (2006) believe that the main cause of a satellite stalling in a constant-density core is that the BPs reaches equilibrium, when they all move along stable epicycles about the satellite with no mean energy and angular momentum transfer to the satellite. The authors observe very low sub-Chandrasekhar exponential decay of the satellite orbit radius in N-body modelling. They suppose this decay to be a consequence of a spurious orbital plane precession due to numerical noise. Gualandris & Merritt (2008) also observe a stage of very low dynamical friction when a radially moving BH sinks into a constant density core (phase II in Gualandris & Merritt 2008). They put forward a hypothesis that the slower damping in this phase is explained by perturbations from individual stars, some of which can accelerate the BH. However, Gualandris & Merritt (2008) do not insist on the explanation of their phase II due to discreteness effects and state that they do not understand the mechanism(s) responsible for the orbital damping in phase II (p. 790 in Gualandris & Merritt 2008). Another point of disagreement is the moment of the onset of stalling. Gualandris & Merritt (2008) argue that the stalling phase begins when the stellar mass interior to the BH orbit is roughly equal to the BH mass (Gualandris & Merritt 2008, section 3.4). Read et al. (2006) note, based on their simulations, that 'the core stalling behaviour is a special property of the harmonic core and not to do with the enclosed mass' (Read et al. 2006, section 4.3). A short stage of enhanced dynamical friction before the stalling stage, which can be seen in almost all numerical simulations, has attracted much less attention from researchers. Read et al. (2006) explain super-Chandrasekhar friction by the equilibrium-orbit transformation. When a satellite nears the constant-density core, stars transit from one set of equilibrium epicycles to the other. This process results in quick energy exchange of the stars with the satellite during approxymately one dynamical time (Read et al. 2006, section 2.2). While having obtained a rather plausible qualitative explanation for the enhanced friction, Read et al. (2006) have not obtained an analytical formula for super-Chandrasekhar dynamical friction force. Some phenomena observed in N-body modelling remain with out any explanation at all. These are stochastic fluctuations of the massive perturber energy at the stalling stage, when its energy is still much greater than the Brownian value (Gualandris & Merritt 2008, fig. 6), and there is evidence of additional frequencies (a kind of beating) at this stage, which can lead to a temporal increase in the perturber energy (Gualandris & Merritt 2008, section 3.4). This observation of Gualandris & Merritt (2008) is very similar to the 'kickback' phenomenon just after the stage of enhanced friction, reported by Goerdt et al. (2010).

In this paper, we try to clarify the physics underlying non-Chandrasekhar dynamical friction in constant-density cores and in initially slightly cuspy distributions, where the massive perturber itself is shown to generate a constant-density core (Goerdt et al. 2010). The main feature of constant-density cores is a nearly harmonic potential at the centre. The period of the unperturbed motion in a purely harmonic potential does not depend on energy and angular momentum, and is the same for all BPs and the perturber. This leads to the resonance of all of the BPs in the core with the massive perturber.

To investigate analytically the interaction of a massive perturber with BPs in constant-density cores, we consider an idealized model of an exactly constant density sphere, surrounded by a vacuum. Without perturbations, the gravitational potential inside the sphere is exactly harmonic, and BPs and the perturber are all in full resonance. In terms of the perturbation theory developed by Tremaine & Weinberg (1984) and Weinberg (1986), this situation corresponds to 'very slow' passing through resonances. So we expect to observe a kind of 'dynamical feedback" of the type modeled by Tremaine & Weinberg (1984). This term means reversible transfer of energy and/or angular momentum from the perturber to BPs. The main differences with the model of Tremaine & Weinberg (1984) are the following: (1) the number of BPs which are in resonance with the perturber at a given time is not infinitesimal, but finite and large. So the back reaction of BPs on the perturber motion is very significant, (2) permanent resonance forces many BPs to enter into a non-linear mode of evolution, and perturbative treatment of BP motion of Tremaine & Weinberg (1984) becomes non-applicable. To solve this problem, non-linear evolution of the particles under the influence of the perturber gravitational field is necessary.

Here we analyse the motion of particles in the harmonic potential under the influence of the Newtonian gravitational field of a point-like massive perturber. As we neglect the back reaction of BPs on the mean potential and consider the perturber orbit to be fixed in zero approximation, the BP equations of motion can be written in a closed form. Read et al. (2006) have previously considered this model and have solved these non-linear equations of motion for each BP numerically, to obtain the evolution of the perturber and BP distribution, which are reported to be consistent with direct N-body results. Our goal is to obtain approximate analytical solutions to these equations, which will allow us to shed more light on the physics of dynamical feedback in constant density cores and to derive a formula for the perturber energy loss at the super-Chandrasekhar stage. We check our analytical results by numerical solution of the BP equations of motion.

The plan of the paper is as follows. In Section 2, we obtain the analytical formula for the frictional force in a constant density sphere. In Section 3, we present the results of numerical simulations and compare them with the analytical results for the first stage of quick energy decay. In Section 4, we discuss features of two more stages after the stage of super-Chandrasekhar friction. At the second stage, the energy of the perturber starts to grow. At the third stage, its energy fluctuates about an approximately constant average value. Section 4.6 contains the discussion of our results in comparison with previous investigations and our conclusions. In the Appendix, we present the derivation of equation (1) to test the method, that is applied to derive the dynamical friction in a constant density spherical star distribution.

2 ANALYTICAL RESULTS

2.1 Model

In order to obtain not only numerical, but also analytical results, we have chosen one of the simplest examples of a highly bound system which is the constant density sphere. This system is a reasonable approximation of real galaxy cores without cusps and has the advantage of analytical solvability. From here on, we refer to the constant density sphere as a galaxy, the BPs as stars and the massive perturber as a BH. However, our results can be equally applied to dark matter particles as the background and to a GC or a galactic bar as the perturber. Orbits of stars in this model are ellipses, all stars have the same period

$$T = \sqrt{\frac{3\pi}{G\rho}}, \tag{2}$$

where ρ is the stellar density Binney & Tremaine (1950). Hence, the stars interact with the BH in a resonant way. This permanent resonant interaction between the BH and the stars is the key difference of our model from that of Chandrasekhar.

We used $\rho = 5.31 \times 10^6\,\mathrm{M_\odot\,kpc^{-3}}$, thus $\omega = 2\pi/T = 10\,\mathrm{Gyr^{-1}}$. Galaxy radius is 1 kpc and mass is $M_\mathrm{g} = 2.22 \times 10^7\,\mathrm{M_\odot}$.

In our model, we put a massive BH (with mass $M \approx 10^{-3} M_\mathrm{g}$) into the constant density sphere of stars. Without the BH, the stars form the quadratic gravitational potential

$$\Phi = \frac{1}{2}\omega^2 r^2,\ \omega^2 = \frac{4}{3}\pi G\rho. \tag{3}$$

The trajectories of the stars in this potential are ellipses with the centres at the centre of the potential:

$$\boldsymbol{r} = \boldsymbol{r}_0 \cos(\omega t) + (\boldsymbol{v}_0/\omega)\sin(\omega t). \tag{4}$$

Without dynamical friction, the BH in the galaxy would have the same trajectory. However, the interaction between a star and the BH changes the trajectories of both bodies. The change of the star trajectories leads to a change in their distribution. We assume that this change in distribution only affects the motion of the BH, and negligibly affects the stars. Thus, we take into consideration only star–BH interactions and neglect star–star interactions, except those of the interaction through the mean gravitational field of the stars.

As we assume that stars always move in quadratic potential, we need, for consistency, to choose the initial star distribution so that the density is constant in space and time in the absence of the BH. The corresponding distribution is

$$f(\boldsymbol{r}, \boldsymbol{v}) = \frac{\rho}{\pi^2\omega^2 R\sqrt{[\boldsymbol{r}\times\boldsymbol{v}]^2 - \omega^2 R^2 r^2 - R^2 v^2 + \omega^2 R^4}}, \tag{5}$$

where R is the ‘radius’ of the galaxy. Integrated over the range of definition, it gives the galaxy mass $M_\mathrm{g} = \frac{4}{3}\pi\rho R^3$.

To get some analytical results, we assume that the BH in zero-order approximation moves with constant energy, just as in Chandrasekhar’s formula derivation. Hence, the trajectory of the BH is only determined by the galaxy initial potential, and the initial velocity and position of the BH. Then we calculate, how much energy is transmitted into stars, and thus we obtain, how quickly the BH loses its energy. The influence of the energy loss on the BH orbit is taken into account afterwards.

2.2 Stellar trajectories

For the chosen system, the unperturbed Hamiltonian is

$$H = \frac{p^2}{2m} + \frac{m\omega^2 r^2}{2}, \tag{6}$$

and the perturbation is

$$V = -GmM/|\boldsymbol{r} - \boldsymbol{R}|. \tag{7}$$

As we assumed that the BH moves in stellar potential only, its trajectory is

$$\boldsymbol{R} = \boldsymbol{R}_0\cos(\omega t) + \frac{\boldsymbol{P}_0}{M\omega}\sin(\omega t). \tag{8}$$

The unperturbed trajectory of a star is

$$\boldsymbol{r} = \boldsymbol{r}_0\cos(\omega t) + \frac{\boldsymbol{p}_0}{m\omega}\sin(\omega t)$$
$$\boldsymbol{p} = \boldsymbol{p}_0\cos(\omega t) - m\boldsymbol{r}_0\omega\sin(\omega t). \tag{9}$$

Putting equation (9) into equations (A2) and (A3) (see the Appendix), taking into account equations (7) and (8), we obtain

$$\cos(\omega t)\dot{\boldsymbol{r}}_0 + \sin(\omega t)\frac{\dot{\boldsymbol{p}}_0}{m\omega} = 0$$
$$-m\omega\sin(\omega t)\dot{\boldsymbol{r}}_0 + \cos(\omega t)\dot{\boldsymbol{p}}_0 = GMm\frac{\partial}{\partial\boldsymbol{r}}\frac{1}{|\boldsymbol{r}-\boldsymbol{R}|}, \tag{10}$$

which can be rewritten in the form

$$\dot{\boldsymbol{a}} = \alpha\frac{\partial}{\partial\boldsymbol{b}}\frac{1}{|\boldsymbol{a}\cos(\omega t) + \boldsymbol{b}\sin(\omega t)|}$$
$$\dot{\boldsymbol{b}} = -\alpha\frac{\partial}{\partial\boldsymbol{a}}\frac{1}{|\boldsymbol{a}\cos(\omega t) + \boldsymbol{b}\sin(\omega t)|}. \tag{11}$$

Here,

$$\alpha = GM/\omega, \tag{12}$$

$$\boldsymbol{a} = \boldsymbol{r}_0 - \boldsymbol{R}_0,$$
$$\boldsymbol{b} = \frac{\boldsymbol{p}_0}{m\omega} - \frac{\boldsymbol{P}_0}{M\omega} \tag{13}$$

are the relative position and normalized velocity of the star in the reference frame of the BH, respectively.

This is a Hamiltonian system with a time-dependent Hamiltonian. Let us assume that during the dynamical time the influence of the BH on the star is small. This is valid for most particles except of those experiencing close encounters with the BH. Their influence is negligible in our model. In this case, we can simplify equation (11) by averaging the Hamiltonian and its arguments over a stellar period. The Averaged Hamiltonian is

$$I(\boldsymbol{a}, \boldsymbol{b}) = \frac{\alpha}{2\pi} \int_0^{2\pi} \frac{\mathrm{d}\zeta}{|\boldsymbol{a}\cos(\zeta) + \boldsymbol{b}\sin(\zeta)|}. \tag{14}$$

As a result, we get a classical Hamiltonian system with time-independent Hamiltonian I:

$$\dot{\boldsymbol{a}} = \frac{\partial I}{\partial \boldsymbol{b}}; \quad \dot{\boldsymbol{b}} = -\frac{\partial I}{\partial \boldsymbol{a}}. \tag{15}$$

As a basic property of such a system, we know that I is constant in time. Also from equation (11), it can easily be derived that the angular momentum in this frame

$$\boldsymbol{L} = [\boldsymbol{a} \times \boldsymbol{b}] \tag{16}$$

is also constant.

Conservation of $\boldsymbol{L}$ leads to the fact that the star's orbit is planar. We choose the plane Oxy so that Ox, Oy and $\boldsymbol{L}$ form a right-hand triple and choose new elliptic variables: q is the major semi-axis, n is the minor semi-axis of the ellipse, θ is the angle between the major semi-axis and Ox and φ is the angle between the radius vector and the major semi-axis. Thus,

$$\boldsymbol{a} = \begin{pmatrix} q\cos\theta\cos\varphi - n\sin\theta\sin\varphi \\ q\sin\theta\cos\varphi + n\cos\theta\sin\varphi \end{pmatrix}$$
$$\boldsymbol{b} = \begin{pmatrix} -q\cos\theta\sin\varphi - n\sin\theta\cos\varphi \\ -q\sin\theta\sin\varphi + n\cos\theta\cos\varphi \end{pmatrix}, \tag{17}$$

$$L = \boldsymbol{L}_z = [\boldsymbol{a} \times \boldsymbol{b}]_z = qn \tag{18}$$

and

$$I = \frac{\alpha}{2\pi} \int_0^{2\pi} \frac{\mathrm{d}\zeta}{\sqrt{q^2\cos^2(\zeta) + n^2\sin^2(\zeta)}} = \frac{2\alpha}{\pi}\frac{1}{q}\mathcal{K}\left(1 - \frac{n^2}{q^2}\right), \tag{19}$$

where $\mathcal{K}(x)$ is the elliptic integral of the first kind. Conservation of $I(q, n)$, $L(q, n)$ leads to conservation of q and n, and therefore to conservation of

$$E = \frac{\boldsymbol{a}^2 + \boldsymbol{b}^2}{2} = \frac{q^2 + n^2}{2}. \tag{20}$$

In these new variables

$$\frac{\partial I}{\partial \boldsymbol{a}} = \frac{\partial I}{\partial q^2}\frac{\partial q^2}{\partial \boldsymbol{a}} + \frac{\partial I}{\partial n^2}\frac{\partial n^2}{\partial \boldsymbol{a}}$$
$$= \left(\frac{\partial I}{\partial q^2} + \frac{\partial I}{\partial n^2}\right)\frac{\partial E}{\partial \boldsymbol{a}} + \left(\frac{\partial I}{\partial q^2} - \frac{\partial I}{\partial n^2}\right)\frac{\partial\sqrt{E^2 - L^2}}{\partial \boldsymbol{a}}$$
$$= \left(\frac{\partial I}{\partial q^2} + \frac{\partial I}{\partial n^2} + \left(\frac{\partial I}{\partial q^2} - \frac{\partial I}{\partial n^2}\right)\frac{E}{\sqrt{E^2 - L^2}}\right)\boldsymbol{a}$$
$$+ \left(\frac{\partial I}{\partial q^2} - \frac{\partial I}{\partial n^2}\right)\frac{L}{\sqrt{E^2 - L^2}}\boldsymbol{b}^{\perp}, \tag{21}$$

where $\boldsymbol{b}^{\perp} = \begin{pmatrix} b_y \\ -b_x \end{pmatrix}$. As E, L, I, q and n conserve,

$$\frac{\partial I}{\partial \boldsymbol{a}} = \Omega_2\boldsymbol{a} - \Omega_1\boldsymbol{b}^{\perp}. \tag{22}$$

Similarly

$$\frac{\partial I}{\partial \boldsymbol{b}} = \Omega_2\boldsymbol{b} + \Omega_1\boldsymbol{a}^{\perp}, \tag{23}$$

where $\boldsymbol{a}^{\perp} = \begin{pmatrix} a_y \\ -a_x \end{pmatrix}$ and

$$\Omega_1 = -\left(\frac{\partial I}{\partial q^2} - \frac{\partial I}{\partial n^2}\right)\frac{L}{\sqrt{E^2 - L^2}},$$
$$\Omega_2 = \frac{\partial I}{\partial q^2} + \frac{\partial I}{\partial n^2} + \left(\frac{\partial I}{\partial q^2} - \frac{\partial I}{\partial n^2}\right)\frac{E}{\sqrt{E^2 - L^2}}. \tag{24}$$

As

$$\mathcal{K}'(x) = \frac{\mathcal{E}(x) - (1 - x)\mathcal{K}(x)}{2(1 - x)x}, \tag{25}$$

where $\mathcal{E}(x)$ is the complete elliptic integral, we can write

$$\frac{\partial I}{\partial q^2} + \frac{\partial I}{\partial n^2} = -\frac{\alpha}{\pi q^2 n^2} n\mathcal{E}\left(1 - \frac{q^2}{n^2}\right),$$
$$\frac{\partial I}{\partial q^2} - \frac{\partial I}{\partial n^2} = \frac{\alpha}{\pi(q^2 - n^2)}$$
$$\times \left(\left(\frac{1}{q^2} + \frac{1}{n^2}\right) n\mathcal{E}\left(1 - \frac{q^2}{n^2}\right) - 2\frac{1}{n}\mathcal{K}\left(1 - \frac{q^2}{n^2}\right)\right). \tag{26}$$

Equations (15) in these new variables (equation 17) take the form:

$$\dot{q} = \dot{n} = 0,$$
$$\dot{\theta} = \Omega_1,$$
$$\dot{\varphi} = \Omega_2. \tag{27}$$

Thus we see that physically orbit averaging in equation (14) is equivalent to the replacement of the true star orbits by precessing ellipses.

Integrating these equations and returning back to the initial variables, we obtain:

$$\boldsymbol{a}(t) = \mathbf{O}_2(t)(\boldsymbol{a}_0\cos(\Omega_2 t) + \boldsymbol{b}_0\sin(\Omega_2 t))$$
$$\boldsymbol{b}(t) = \mathbf{O}_2(t)(-\boldsymbol{a}_0\sin(\Omega_2 t) + \boldsymbol{b}_0\cos(\Omega_2 t)), \tag{28}$$

where

$$\boldsymbol{a}_0 = \boldsymbol{r}(0) - \boldsymbol{R}(0)$$
$$\boldsymbol{b}_0 = \frac{1}{m\omega}\boldsymbol{p}(0) - \frac{1}{M\omega}\boldsymbol{P}(0), \tag{29}$$

and $\mathbf{O}_2(t)$ is a 2D rotation matrix:

$$\mathbf{O}_2(t) = \begin{pmatrix} \cos(\Omega_1 t) & -\sin(\Omega_1 t) \\ \sin(\Omega_1 t) & \cos(\Omega_1 t) \end{pmatrix}. \tag{30}$$

To rewrite these equations for an arbitrary orbit plane, we need to replace the matrix $\mathbf{O}_2(t)$ with the 3D rotational matrix $\mathbf{O}(t)$ on the angle $\theta = \Omega_1 t$ around $\boldsymbol{n} = \boldsymbol{L}/L$ (equation A19).

Therefore, the star trajectory is

$$\boldsymbol{r}(t) = \mathbf{O}(t)(\boldsymbol{a}_0\cos(\omega' t) + \boldsymbol{b}_0\sin(\omega' t)) + \boldsymbol{R}(t)$$
$$\boldsymbol{p}(t) = m\omega\mathbf{O}(t)(-\boldsymbol{a}_0\sin(\omega' t) + \boldsymbol{b}_0\cos(\omega' t)) + \frac{m}{M}\boldsymbol{P}(t), \tag{31}$$

where

$$\omega' = \omega + \Omega_2. \tag{32}$$

Equation (31) reveals how stellar trajectories change under the influence of the BH. First of all, stellar orbital frequencies are changed, and they are not the same as that of the BH.

Secondly, rotational matrix $\mathbf{O}(t)$ causes a slow precession of the star's orbit with the frequency Ω_1.

As we see, the star orbits are indeed stable epicycles in the BH frame of reference, as it has been stated by Read et al. (2006). The orbit is characterized by two more frequencies Ω_1 and Ω_2. They are both typically much less than the dynamical frequency ω: $\Omega_1 \sim \Omega_2 \sim \frac{M}{M_g}\omega \sim 10^{-3}\omega$. Physically Ω_1 determines the frequency of the orbit pericentre precession in the BH reference frame. It determines the evolution of the BH wake shape and position and thus governs the energy flux from the BH to stars. Ω_2 gives a small drift of the star orbital phase. After averaging over star distribution, this phase drift does not influence the net energy flux.

Having obtained the star trajectory (equation 31) we are able to study the energy exchange between the BH and the stars.

2.3 Energy exchange

The dependence of the stellar energy $e = \frac{p^2}{2m} + \frac{m\omega^2 r^2}{2}$ on time can be derived directly from equation (31):

$$\begin{aligned} e(t) = e(0) & + m\omega^2 R_0^2(1 - \cos\varphi_r \cos(\Omega_2 t)) - m(\omega \boldsymbol{r}_0 \cdot \omega \boldsymbol{R}_0) \\ & + m((\omega \boldsymbol{r}_0 \cos(\Omega_2 t) + \boldsymbol{v}_0 \sin(\Omega_2 t)) \cdot \mathbf{O}(t)\omega \boldsymbol{R}_0) \\ & + m V_0^2(1 - \cos\varphi_v \cos(\Omega_2 t)) - m(\boldsymbol{v}_0 \cdot \boldsymbol{V}_0) \\ & + m((\boldsymbol{v}_0 \cos(\Omega_2 t) - \omega \boldsymbol{r}_0 \sin(\Omega_2 t)) \cdot \mathbf{O}(t)\boldsymbol{V}_0), \end{aligned} \tag{33}$$

where

$$\cos\varphi_i = \cos^2\gamma_i + \sin^2\gamma_i \cos(\Omega_1 t), \tag{34}$$

γ_r is the angle between $\boldsymbol{R}_0$ and $\boldsymbol{L} = [\boldsymbol{a}_0 \times \boldsymbol{b}_0]$, γ_v is the angle between $\boldsymbol{V}_0$ and $\boldsymbol{L}$, and $\boldsymbol{V}_0 = \boldsymbol{P}(0)/M$. We have neglected the potential energy of star–BH interaction, because we assume it to be much less than the star-galaxy one.

Energy transfer from the BH to a single star is therefore defined as

$$\begin{aligned} \dot{e}(t) = & \, m\Omega_2\omega^2 R_0^2 \cos\varphi_r \sin(\Omega_2 t) + m\Omega_2 V_0^2 \cos\varphi_v \sin(\Omega_2 t) \\ & + m\Omega_1\omega^2 R_0^2 \sin^2\gamma_r \sin(\Omega_1 t)\cos(\Omega_2 t) \\ & + m\Omega_1 V_0^2 \sin^2\gamma_v \sin(\Omega_1 t)\cos(\Omega_2 t) \\ & + m((\omega \boldsymbol{r}_0 \cos(\Omega_2 t) + \boldsymbol{v}_0 \sin(\Omega_2 t)) \cdot \dot{\mathbf{O}}(t)\omega \boldsymbol{R}_0) \\ & + m((\boldsymbol{v}_0 \cos(\Omega_2 t) - \omega \boldsymbol{r}_0 \sin(\Omega_2 t)) \cdot \dot{\mathbf{O}}(t)\boldsymbol{V}_0) \\ & + m\Omega_2((\boldsymbol{v}_0 \cos(\Omega_2 t) - \omega \boldsymbol{r}_0 \sin(\Omega_2 t)) \cdot \mathbf{O}(t)\omega \boldsymbol{R}_0) \\ & + m\Omega_2((\omega \boldsymbol{r}_0 \cos(\Omega_2 t) + \boldsymbol{v}_0 \sin(\Omega_2 t)) \cdot \mathbf{O}(t)\boldsymbol{V}_0). \end{aligned} \tag{35}$$

The total energy loss of the BH is the sum of energies transmitted from the BH to every star. If we replace the sum by the integral over the phase space, we get

$$\begin{aligned} \dot{E}_{\rm bh}(t) = -\rho \int & \{\Omega_2\omega^2 R_0^2 \cos\varphi_r \sin(\Omega_2 t) \\ & + \Omega_2 V_0^2 \cos\varphi_v \sin(\Omega_2 t) \\ & + \Omega_1\omega^2 R_0^2 \sin^2\gamma_r \sin(\Omega_1 t)\cos(\Omega_2 t) \\ & + \Omega_1 V_0^2 \sin^2\gamma_v \sin(\Omega_1 t)\cos(\Omega_2 t) \\ & + ((\omega \boldsymbol{r}_0 \cos(\Omega_2 t) + \boldsymbol{v}_0 \sin(\Omega_2 t)) \cdot \dot{\mathbf{O}}(t)\omega \boldsymbol{R}_0) \\ & + ((\boldsymbol{v}_0 \cos(\Omega_2 t) - \omega \boldsymbol{r}_0 \sin(\Omega_2 t)) \cdot \dot{\mathbf{O}}(t)\boldsymbol{V}_0) \\ & + \Omega_2((\boldsymbol{v}_0 \cos(\Omega_2 t) - \omega \boldsymbol{r}_0 \sin(\Omega_2 t)) \cdot \mathbf{O}(t)\omega \boldsymbol{R}_0) \\ & + \Omega_2((\omega \boldsymbol{r}_0 \cos(\Omega_2 t) + \boldsymbol{v}_0 \sin(\Omega_2 t)) \cdot \mathbf{O}(t)\boldsymbol{V}_0)\} \\ & \times f(\boldsymbol{r}, \boldsymbol{v}) \mathrm{d}^3\boldsymbol{r} \mathrm{d}^3\boldsymbol{v}. \end{aligned} \tag{36}$$

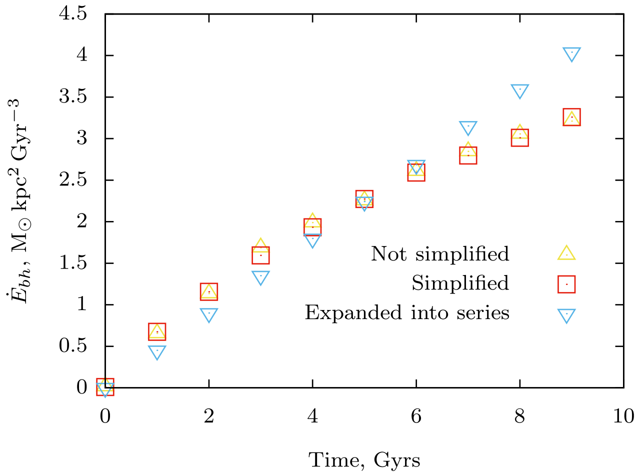

Figure 1. The BH energy loss according to the Monte Carlo integration for: not simplified equation (36), simplified equation (42) and equation with sine expanded into series (47) for $|X_1| = |X_2| = 1/\sqrt{2}$, $X_1 \perp X_2$. This shows that assumptions made to derive the resulting formula (47) are correct. $M_g = 10^3$, $M = 1$, $\omega = 1$, $R_g = 1$.

As we consider the motion averaged over the orbital period, the orbital phase distribution can be considered to be uniform. This means that equation (36) cannot depend on the orbital phase shift $\Omega_2 t$. Neglecting the phase shift by assuming $\Omega_2 = 0$, we can simplify this equation as follows:

$$\begin{aligned} \dot{E}_{\rm bh}(t) = -\rho \int & \{\Omega_1\omega^2 R_0^2 \sin^2\gamma_r \sin(\Omega_1 t) \\ & + \Omega_1 V_0^2 \sin^2\gamma_v \sin(\Omega_1 t) + \omega^2(\boldsymbol{r}_0 \cdot \dot{\mathbf{O}}(t)\boldsymbol{R}_0) \\ & + (\boldsymbol{v}_0 \cdot \dot{\mathbf{O}}(t)\boldsymbol{V}_0)\} f(\boldsymbol{r}, \boldsymbol{v}) \mathrm{d}^3\boldsymbol{r} \mathrm{d}^3\boldsymbol{v}. \end{aligned} \tag{37}$$

The integral in this equation consists of two parts, proportional to $\sin\Omega_1 t$ (let us denote it as $\dot{E}_{{\rm bh},sin}(t)$) and to $\cos\Omega_1 t$:

$$\begin{aligned} \dot{E}_{\rm bh}(t) = \dot{E}_{{\rm bh},sin}(t) + \rho \int & [\omega^2(\boldsymbol{r} \cdot [\boldsymbol{R}_0 \times \boldsymbol{n}]) + (\boldsymbol{v} \cdot [\boldsymbol{V}_0 \times \boldsymbol{n}])] \\ & \times \cos(\Omega_1 t) f(\boldsymbol{r}, \boldsymbol{v}) \mathrm{d}^3\boldsymbol{r} \mathrm{d}^3\boldsymbol{v}. \end{aligned} \tag{38}$$

As the trajectory is averaged over the period (equation 14), we can move the stars and the BH forward in a quarter of a period. This changes $\boldsymbol{R}_0 \to \boldsymbol{V}_0/\omega$, $\boldsymbol{V}_0 \to -\omega\boldsymbol{R}_0$, $\boldsymbol{r} \to \boldsymbol{v}/\omega$, $\boldsymbol{v} \to -\omega\boldsymbol{r}$. But due to symmetry, we can change $\boldsymbol{R}_0 \to -\boldsymbol{R}_0$, $\boldsymbol{V}_0 \to -\boldsymbol{V}_0$, $\boldsymbol{r} \to -\boldsymbol{r}$, $\boldsymbol{v} \to -\boldsymbol{v}$. These two changes invert the sign of the second term, but this does not change the result. Therefore, the second term in equation (38) is zero. A similar argument is valid for any chosen $\Omega_2 t$ value.

These simplifications are confirmed by numerical calculations (see Fig. 1). Then we have:

$$\begin{aligned} \dot{E}_{\rm bh}(t) = -\rho \int & \Omega_1[V_0^2 \sin^2\gamma_v + (\boldsymbol{v_0} \cdot \boldsymbol{n})(\boldsymbol{V_0} \cdot \boldsymbol{n}) \\ & - (\boldsymbol{v_0} \cdot \boldsymbol{V_0}) + \omega^2(R_0^2 \sin^2\gamma_r + (\boldsymbol{r_0} \cdot \boldsymbol{n})(\boldsymbol{R_0} \cdot \boldsymbol{n}) - (\boldsymbol{r_0} \cdot \boldsymbol{R_0}))] \\ & \times \sin(\Omega_1 t) f(r, v) \mathrm{d}^3\boldsymbol{r} \mathrm{d}^3\boldsymbol{v}, \end{aligned} \tag{39}$$

where $\boldsymbol{n} = \boldsymbol{L}/L$, $\boldsymbol{L} = [\boldsymbol{a} \times \boldsymbol{b}]$, or, finally,

$$\dot{E}_{\rm bh}(t) = \rho \int \Omega_1 \{([\boldsymbol{V_0} - \boldsymbol{v_0} \times \boldsymbol{n}] \cdot [\boldsymbol{V_0} \times \boldsymbol{n}] + \omega^2([\boldsymbol{R_0} - \boldsymbol{r_0} \times \boldsymbol{n}] \cdot [\boldsymbol{R_0} \times \boldsymbol{n}])) \sin(\Omega_1 t) f(r, v)\} \mathrm{d}^3\boldsymbol{r}\mathrm{d}^3\boldsymbol{v}. \tag{40}$$

To explore the dependence of this result on system parameters, we convert this equation to the dimensionless form. Let the radius of the galaxy be $R_{\rm g}$, then

$$\boldsymbol{r} = R_{\rm g}\boldsymbol{x_1}$$

$$\boldsymbol{v} = R_{\rm g}\omega\boldsymbol{x_2}$$

$$\boldsymbol{R_0} = R_{\rm g}\boldsymbol{X_1}$$

$$\boldsymbol{V_0} = R_{\rm g}\omega\boldsymbol{X_2}$$

$$f(\boldsymbol{x_1}, \boldsymbol{x_2})\mathrm{d}^3\boldsymbol{x_1}\mathrm{d}^3\boldsymbol{x_2} = \frac{f(R_{\rm g}\boldsymbol{x_1}, R_{\rm g}\omega\boldsymbol{x_2})}{4/3\pi R_{\rm g}^3}\mathrm{d}^3\boldsymbol{r}\mathrm{d}^3\boldsymbol{v}, \tag{41}$$

so the transmitted energy is

$$\dot{E}_{\rm bh}(t) = M_{\rm g} R_{\rm g}^2\omega^2 \int \{\Omega_1([\boldsymbol{X_1} - \boldsymbol{x_1} \times \boldsymbol{n}] \cdot [\boldsymbol{X_1} \times \boldsymbol{n}]) + ([\boldsymbol{X_2} - \boldsymbol{x_2} \times \boldsymbol{n}] \cdot [\boldsymbol{X_2} \times \boldsymbol{n}])\} \sin(\Omega_1 t) f(\boldsymbol{x_1}, \boldsymbol{x_2}) \mathrm{d}^3\boldsymbol{x_1}\mathrm{d}^3\boldsymbol{x_2}, \tag{42}$$

and

$$\Omega_1 = -\omega\frac{M}{M_{\rm g}}\frac{2q'n'}{\pi(q'^2 - n'^2)^2} \times \left(\left(\frac{1}{q'^2} + \frac{1}{n'^2}\right)n'\mathcal{E}\left(1 - \frac{q'^2}{n'^2}\right) - 2\frac{1}{n'}\mathcal{K}\left(1 - \frac{q'^2}{n'^2}\right)\right), \tag{43}$$

where

$$q = R_{\rm g}q'$$

$$n = R_{\rm g}n', \tag{44}$$

and

$$\frac{M}{M_{\rm g}} = \frac{GM}{\frac{4}{3}\pi G\rho R_{\rm g}^3} = \frac{GM}{\omega^2 R_{\rm g}^3} = \frac{\alpha}{R_{\rm g}^3\omega}. \tag{45}$$

Thus,

$$\Omega_1 = -\omega\frac{M}{M_{\rm g}}Q(q', n'), \tag{46}$$

where $Q(q', n')$ is a dimensionless function. This function is singular in $q' = 0$, $n' = 0$ (which corresponds to the close interactions between a star and the BH) or $q' = n'$, but it is nearly of the order of 1 for average q' and n' in our system. In our model the value of $M/M_{\rm g}$ is about 10^{-3}. Therefore, Ω_1 is about $10^{-3}\omega$ for most stars. This is a slow frequency of star trajectory change. Therefore for times $t \ll \frac{M_{\rm g}}{M}T$, where T is the orbital period, the sine in equation (42) can be replaced by the Taylor series. As shown further, if the initial velocity of the BH is about the escape velocity[1] of the galaxy and E_0 is about $R_{\rm g}^2\omega^2$, the time required for the BH to lose all of its energy is about the same value.

[1] Here and after we use the term 'escape velocity' for the velocity of the BH required to reach the border of the galaxy from the centre, not the velocity required to reach infinity. So $V_{\rm esc} = \omega R_{\rm g}$.

Fig. 1, shows the results of Monte Carlo integration for equations (36) and (42) and equation:

$$\dot{E}_{\rm bh}(t) = \frac{R_{\rm g}^2 M^2\omega^4 t}{M_{\rm g}} \int' \{([\boldsymbol{X_1} - \boldsymbol{x_1} \times \boldsymbol{n}] \cdot [\boldsymbol{X_1} \times \boldsymbol{n}]) + ([\boldsymbol{X_2} - \boldsymbol{x_2} \times \boldsymbol{n}] \cdot [\boldsymbol{X_2} \times \boldsymbol{n}])\} Q^2(q', n') \times f(\boldsymbol{x_1}, \boldsymbol{x_2})\mathrm{d}^3\boldsymbol{x_1}\mathrm{d}^3\boldsymbol{x_2}, \tag{47}$$

where $'$ over the integral means that the regions where $Q(q', n') \gg 1$ are excluded from the integration. The integral depends only on $\boldsymbol{X_1}$ and $\boldsymbol{X_2}$, so we can write:

$$\dot{E}_{\rm bh}(t) = -\frac{R_{\rm g}^2 M^2\omega^4 t}{M_{\rm g}}F(\boldsymbol{X_1}, \boldsymbol{X_2}). \tag{48}$$

As $E_{\rm bh} = MV_0^2/2 + M\omega^2 R_0^2/2 = MR_{\rm g}^2\omega^2\left(X_1^2 + X_2^2\right)/2$,

$$\frac{\dot{E}_{\rm bh}(t)}{E_{\rm bh}} = -2\frac{M}{M_{\rm g}}\frac{F(\boldsymbol{X_1}, \boldsymbol{X_2})}{X_1^2 + X_2^2}\omega^2 t. \tag{49}$$

Results of Monte Carlo calculations of the dimensionless expression

$$\frac{F(\boldsymbol{X_1}, \boldsymbol{X_2})}{X_1^2 + X_2^2}, \tag{50}$$

shown in Fig. 2, reveal that this value has very small variations and can be replaced by a constant C:

$$\frac{F(\boldsymbol{X_1}, \boldsymbol{X_2})}{X_1^2 + X_2^2} \approx C \approx 2. \tag{51}$$

Precise value of C depends almost logarithmically on the value of $\Omega'_{1\max}$. In our calculations, we used $\Omega'_1 < 3$. Below we show that the value $C \approx 2$ is consistent with numerical calculations.

So we have

$$\frac{\dot{E}_{\rm bh}(t)}{E_{\rm bh}} = -2C\frac{M}{M_{\rm g}}\omega^2 t. \tag{52}$$

and

$$E_{\rm bh}(t) = E_0 \exp\left[-C\frac{M}{M_{\rm g}}\omega^2 t^2\right]. \tag{53}$$

This integration is valid assuming that the energy of the BH changes more slowly than star–BH interaction is established which is proved by numerical calculations.

One of the most interesting consequences of this equation is that for the same initial velocity (relative to the escape velocity) the BH loses its energy in

$$N \propto \sqrt{M_{\rm g}/M} \tag{54}$$

oscillations.

So we obtain that in a constant density core the dynamical friction force due to resonant interaction with stars is $(M/M_{\rm g})^{-1/2}$ times stronger than the usual Chandrasekhar friction, caused by pair encounters. The same difference by the factor $(M/M_{\rm g})^{-1/2}$ was obtained by Tremaine & Weinberg (1984, in their section 3.3) between usual friction and 'dynamical feedback'. Hence, we can believe that super-Chandrasekhar friction is the same phenomenon as the 'dynamical feedback' of Tremaine & Weinberg, connected with the slow passage of a massive satellite through resonance with stars. Indeed, in our model with harmonic potential all stars of this constant density core are in permanent resonance with the BH.

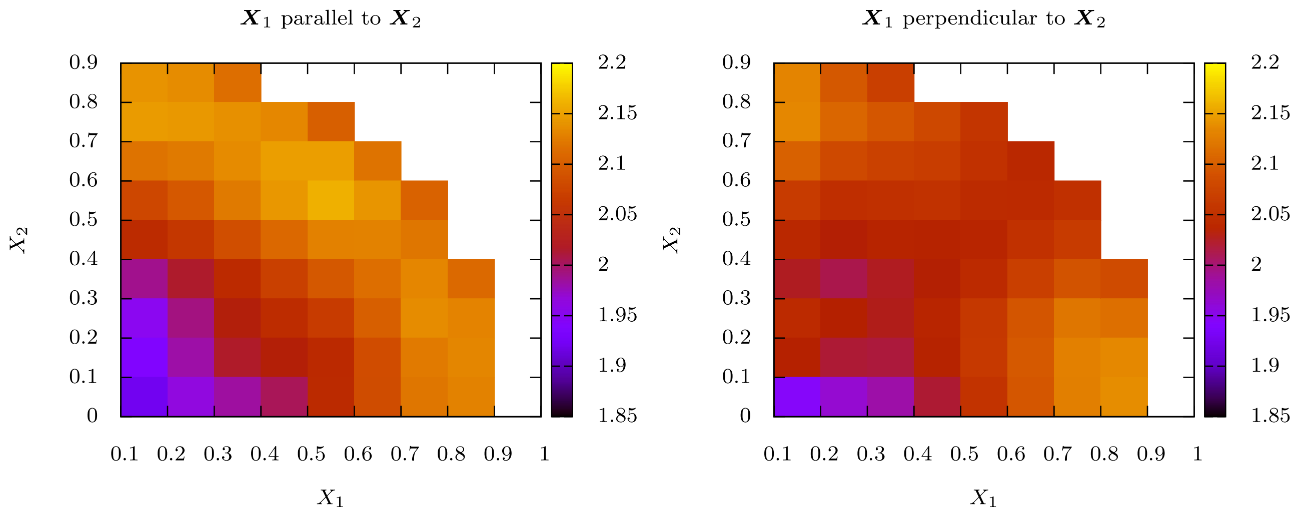

Figure 2. Expression (50) calculated for different X_1 and X_2. The results are Monte Carlo integrations with distribution (5) over 10^7 stars. This shows that there is almost no dependence of BH's energy decay on its initial position $\boldsymbol{R}_0 = R_{\rm g} X_1$ and velocity $\boldsymbol{V}_0 = \omega R_{\rm g} X_1$. The total deviation from the constant is less than 10 per cent.

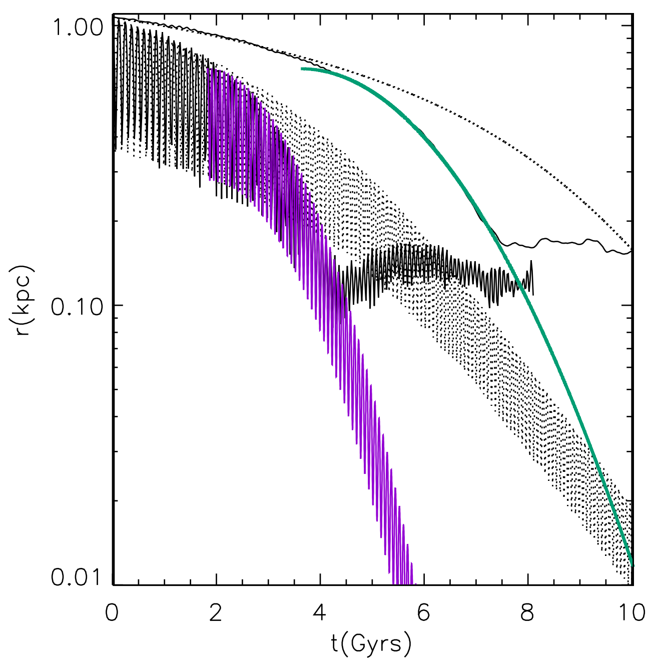

Figure 3. Numerical simulations from Read et al. (2006) as compared with our theoretical fit. Caption of fig. 3 from the paper of Read et al. (2006): 'The decay of the radius of the GC as a function of time for a GC on a circular (straight solid line) and elliptical (oscillating solid line) orbit.' Dotted lines are Chandrasekhar's estimates. Coloured lines are our analytical fits of the super-Chandrasekhar phase with equation (55).

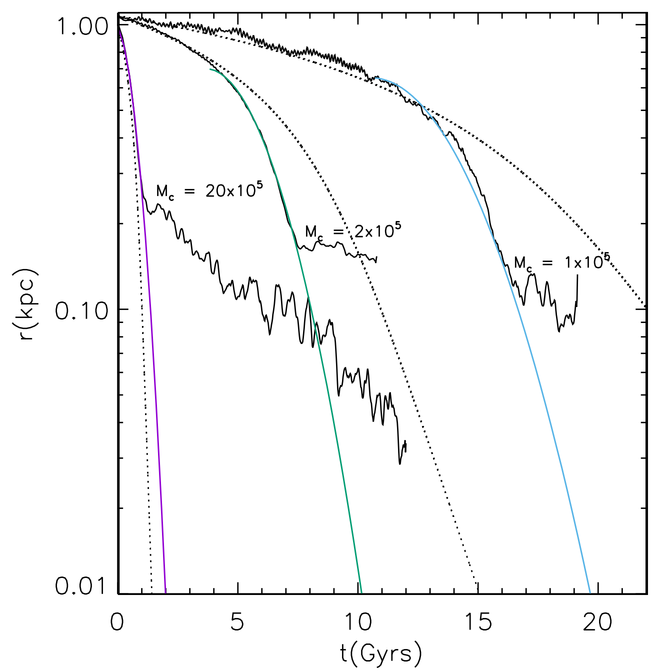

Figure 4. Numerical simulations from Read et al. (2006) as compared with our theoretical fit. Caption of fig. 5 from the paper of Read et al. (2006): 'The decay rate of the GC as a function of $M_{\rm c}$...'. Bold solid are experimental lines from the paper, bold dotted lines are their Chandrasekhar fit and coloured lines are our analytical fits of the super-Chandrasekhar phase with equation (55).

This result can be compared with the numerical calculations of Read et al. (2006). The amplitude of the GC oscillation in this paper can be fitted with our formula

$$r_{\rm bh}, \max(t) = r_0 \exp\left[-\frac{1}{2} C \frac{M}{M_{\rm g}} \omega^2 t^2\right]. \tag{55}$$

We fit only the non-Chandrasekhar phase of the radius decay function of the GC. The results are shown in Fig. 3. The numerical factor in the exponent corresponds to the ratio $M/M_{\rm g}$ about 0.5×10^{-4} and 1.5×10^{-4}. The exact value from the paper of Read et al. (2006) is $M/M_{\rm g} = 10^{-4}$. In Fig. 4 there are fits for simulations of Read et al. (2006) for various GC masses. Fig. 5 shows a similar simulation of Goerdt et al. (2006) compared with our analytical data. Fig. 6 shows a comparison with the simulation of Gualandris & Merritt (2008)

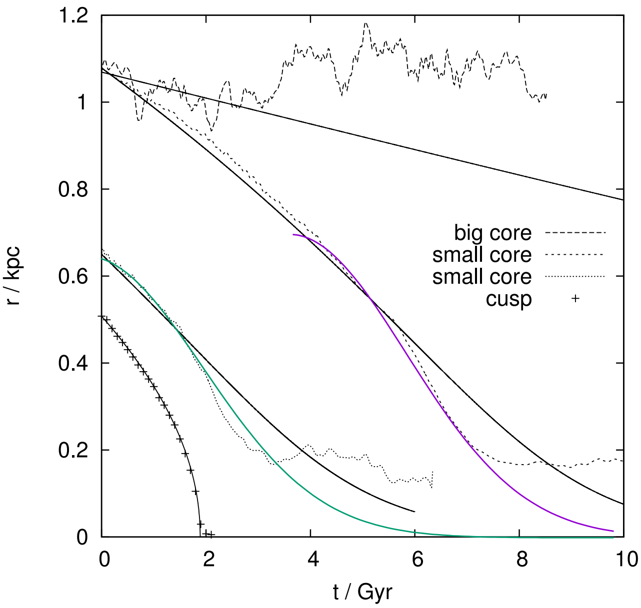

Figure 5. Numerical simulations from Goerdt et al. (2006) as compared with our theoretical fit. Caption of fig. 2 from the paper of Goerdt et al. (2006): 'Radial distance of the single globular cluster from the centre of its host halo as a function of time. We start the calculations with the globular at different initial radii for clarity. Solid curves are the analytic estimates, dashed curves are from the numerical simulations.' Coloured lines are our analytical fits of the super-Chandrasekhar phase with equation (55).

3 NUMERICAL CALCULATION

To check our analytical formula (53) for super-Chandrasekhar dynamical friction we use not the usual N-body simulation but a kind of a simplified numerical calculation.

3.1 Calculation algorithm

The model of numerical calculation was chosen to be close to the analytical one. The spherical field was filled with stars of the same mass according to distribution (equation 5). The BH was put in the centre of this sphere with an initial velocity equal to or less than the escape velocity. To simplify the calculation, star–star interactions were replaced by the interaction with the mean star potential, which was considered to be stationary, hailed and equal to equation (3). This reduces the difficulty of the calculation from $O(N^2)$ to $O(N)$. During the calculation, the integration step was chosen to provide a relative error of 10^{-5} at every step. When a star get too close to the BH so that the integration step becomes smaller than 10^{-10}, then the galaxy potential was ignored and the star was moved analytically relative to the BH using Kepler's orbit (Bate, Mueller & White 1971). This algorithm has also been previously applied by Lezhnin & Chernjagin (2014).

The absence of the effects produced by numerical errors was checked by test calculations with better precision. A number of calculations were completed using three different initial steps, each five times smaller than the other and the calculation results showed no dependence on the integration step.

The initial star distribution was generated using Monte Carlo method according to equation (5). After the initial distribution

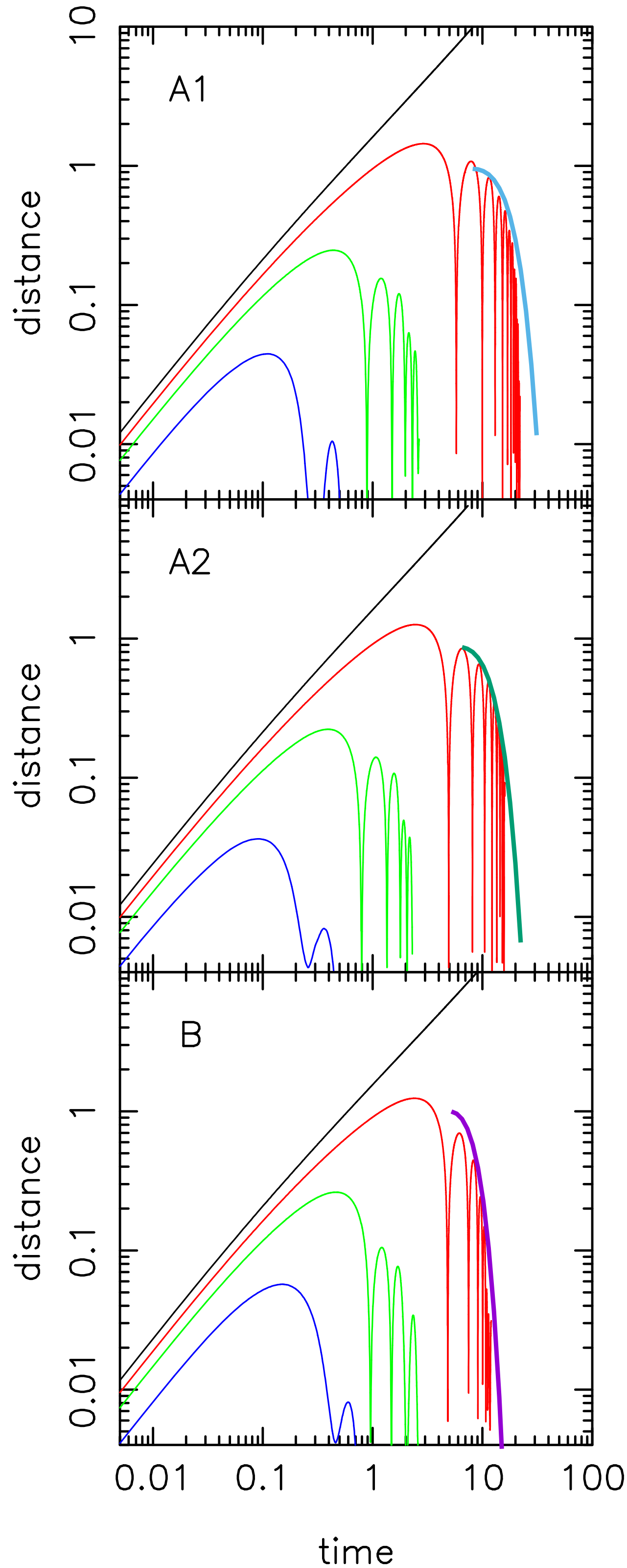

Figure 6. Numerical simulations from Gualandris & Merritt (2008) as compared with our theoretical fit. Bold coloured lines are our analytical fits of the super-Chandrasekhar phase with equation (55) according to BH masses described in the paper.

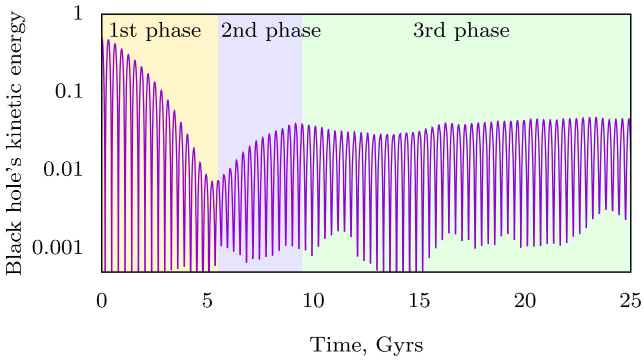

Figure 7. Evolution of the BH's kinetic energy. $M = 10^{-3}M_g$, $m_{star} = 10^{-6}M_g$.

was generated, some stars were replaced to ensure the following conditions:

$$m\omega\left|\sum \boldsymbol{r_0}\right| < 10^{-3}MV_0$$

$$\left|m\sum \boldsymbol{v_0} + M\boldsymbol{V_0}\right| < 10^{-3}MV_0$$

$$m\omega\left|\sum[\boldsymbol{r_0}\times\boldsymbol{v_0}]\right| < 10^{-3}MV_0^2. \quad (56)$$

These conditions are required to avoid additional artificial oscillation and rotation of the BH due to discrete effects in a system without such a large number of stars. The problem is that a random distribution of the given number of stars (10^5–10^6) has its centre of mass at $R_c \sim R_g/\sqrt{N}$ on average, while the potential is 'pinned' at zero-point. In addition, non-zero random net angular momentum of the stars can cause artificial rotation of the BH.

After all, the BH was placed in the middle of the galaxy with initial speed V_0.

As a result, this model has three parameters: initial velocity of the BH, the galaxy mass and the star mass. BH mass is taken as 1. Time is normalized so that $\omega = 1$.

3.2 Results of the calculation

Calculations were made for various BH masses, initial velocities, and star masses. As an example, Fig. 7 shows the dependence of the kinetic energy[2] of the bh on time for $M = 10^{-3}M_g$, $m = 10^{-6}M_g$ and $V_0 = V_{esc}$.

The motion of the BH can be divided into three phases: the first is fairly rapid damping, the second is symmetric rapid acceleration and the third is oscillations with almost constant average amplitude.

The first phase is well described by equation (53). In Fig. 8, you can see the first phase of motion for various initial conditions and the results, predicted by equation (53). The value of C used for fitting is represented in the figure. Fig. 9 shows the time needed for the BH to lower its energy down to 0.02 of the initial value as a function of the its mass. We see excellent agreement with the analytical formula (54).

The first phase ends when the energy of the BH reaches approximately the Brownian energy.

[2] BH's energy in this section is always normalized to the value of $MR_g\omega^2$.

4 DISCUSSION OF THE RESULTS

4.1 Initial time dependence

In Chandrasekhar's case, the motion of the BH is stationary, so the wake mass and the friction not depend on time. In our model at the beginning the wake is absent, and the friction is zero. Oscillations of the BH leads to the formation of a wake, oscillating with the same frequency in antiphase with the BH. Its mass grows linearly (see Fig. 10), giving rise to the time dependence of the right-hand side of equation (52).

4.2 Super-Chandrasekhar's friction

Adapting Chandrasekhar's formula (1) to our model and taking $\rho(<V) = \rho\frac{V^3}{\omega^3 R_g^3}$, we have

$$\frac{dV}{dt} = -3\ln\Lambda\frac{M}{M_g}\omega V, \quad (57)$$

or, integrating and assuming $C = -6\ln\Lambda$, we get

$$E_{bh}(t) = E_0\exp\left[-C\frac{M}{M_g}\omega t\right]. \quad (58)$$

This equation means that typical time of Chandrasekhar's energy decay would be

$$T \approx \frac{M_g}{M}\omega^{-1}. \quad (59)$$

In our model, the typical time is

$$T \approx \sqrt{\frac{M_g}{M}}\omega^{-1}. \quad (60)$$

So, in a constant density core the energy decay of the BH is half an order in the BH mass faster than in Chandrasekhar's formula. This is the result of all stars being resonant to the BH.

In her paper, Colpi (1998) describes the motion of a satellite, orbiting the spherical galaxy with quadratic potential. Her analytical results applied to the particular case of the satellite and stars moving with the same period as shown in equation (60) a power dependence of the damping time on the satellite mass with power 0.5 (or 0.4 numerically).

A short super-Chandrasekhar phase can also be distinguished between Chandrasekhar and sub-Chandrasekhar stages in the paper of Gualandris & Merritt (2008), but the authors do not pay much attention to it.

It should be noted that if the initial speed of the BH is more than V_{esc}, then the BH spends some time outside the galaxy and its period becomes longer than $2\pi/\omega$. This causes the BH to lose resonance with other stars. In this case, the wake survives only during half of a single period, because it moves with a period, that is different from that of the BH. The decay time in this regime is given by Chandrasekhar's value equation (59) rather than by equation (60). This situation only corresponds to the first (Chandrasekhar) stage of the BH motion in the paper of Gualandris & Merritt (2008).

4.3 Energy growth

From Figs 7 and 8 we see that when the energy of the BH lowers to approximately Brownian level

$$\frac{1}{2}MV^2 \sim \frac{1}{2}mv^2. \quad (61)$$

a symmetric energy growth begins. It has almost the same rate, but shorter duration. Energy does not return to the initial value and stops

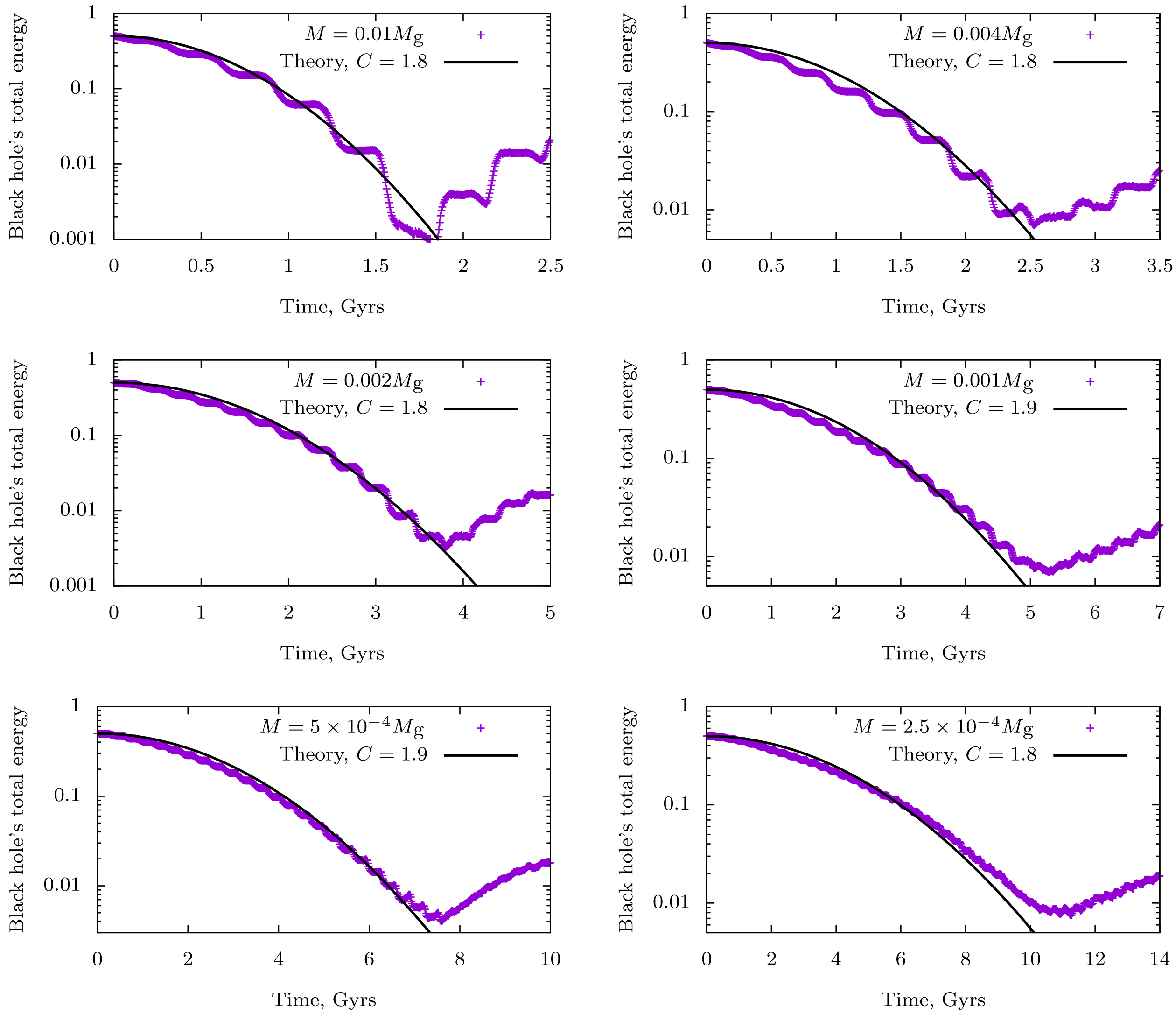

Figure 8. Numerical calculations and theoretical curve (equation 53) for different BH masses, $m_{\mathrm{star}} = 10^{-3}M$.

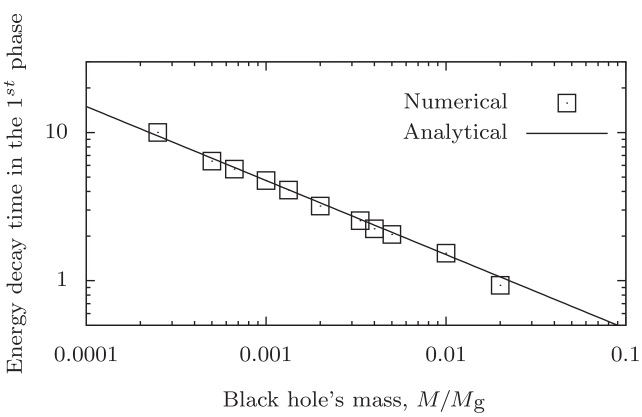

Figure 9. Energy decay time of the BH to the level of 0.02 of the initial energy (boxes) and the same time predicted by the theoretical equation (54) (line).

at a level an order of magnitude higher than the Brownian energy. This 'kickback' effect has been first reported by Goerdt et al. (2010).

In the third phase, the energy of the BH fluctuates randomly with almost constant average amplitude. This amplitude does not depend on the initial star realization (see Fig. 11) or on a single star mass m (Fig. 12), so the effect of zero friction is not caused by the interaction with single stars.

Dependence of the third stage energy on the BH mass is shown in Fig. 13. There seems to be no evident dependence. This means that this effect is caused by the fact that after a slight distribution change there appears a quasi-stationary orbit inside the sphere, where average energy exchange with stars is absent. This orbit is fully determined by the new distribution, and, therefore, does not depend on the BH mass (which is simply the parameter defining speed of interaction).

Dependence of the third stage energy on the initial energy of the BH is shown in Fig. 14.

We can try to understand this unexpected phenomenon through the consideration of the BH wake behaviour. For radial oscillations of the BH wake oscillates in the antiphase initially. As the amplitude

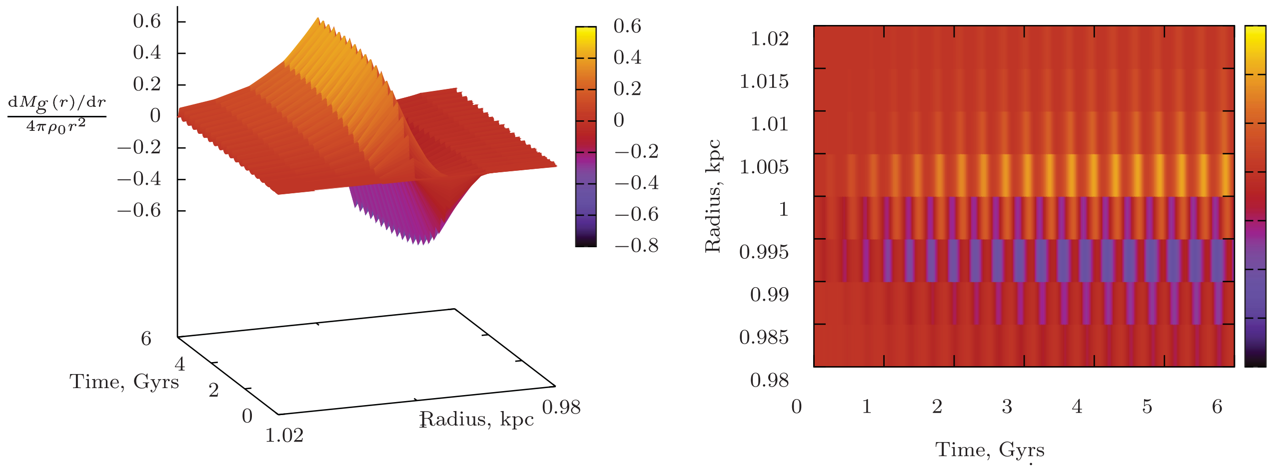

Figure 10. Time-dependent 'wake' near the outer edge of the star distribution. Only narrow region near the border of the sphere is shown where the density change is the highest. High and low density at the edge alternate depending on the direction of the motion of the black hole. Relative density change is shown in colour.

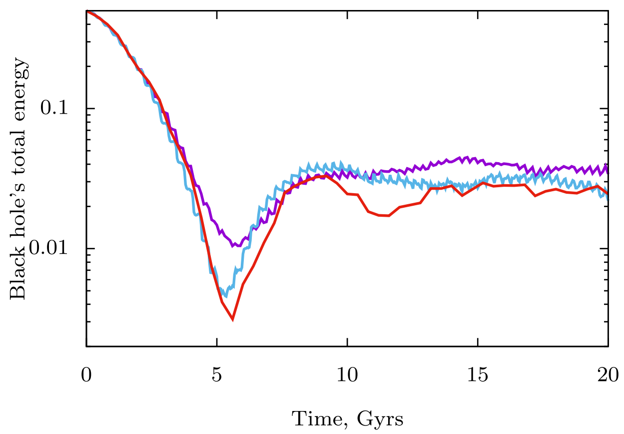

Figure 11. Dependence of the third-phase energy on realization. Three lines show the BH's total energy as a function of time for three different initial star distributions with the same mean parameters $M = 10^{-3}M_g$, $m_{star} = 10^{-6}M_g$.

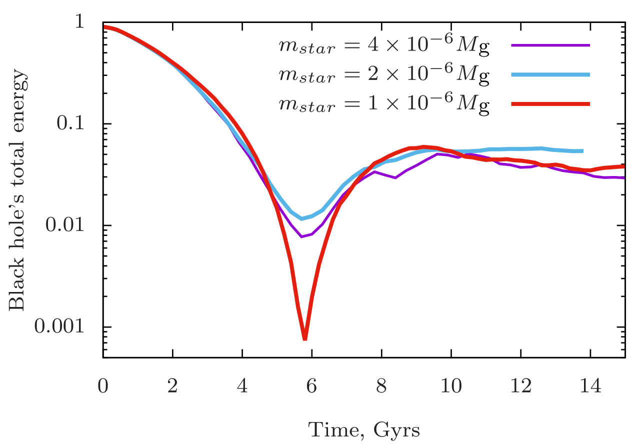

Figure 12. Dependence of the third-phase energy on the mass of the star. $M = 10^{-3}M_g$.

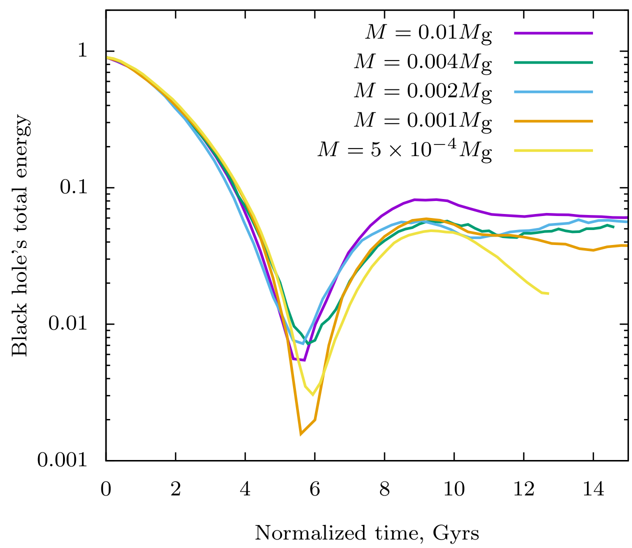

Figure 13. Dependence of the third-phase energy on the BH mass. $m_{star} = 10^{-3}M$. Time is normalized according to equation (54) by the value of $\sqrt{M_g/10^3 M}$, so that the first stage would be the same for all curves.

of the BH oscillations decreases, the phase shift between the wake and the BH changes, and finally the wake starts to accelerate the BH.

4.4 Loss of friction

After the end of the first phase of energy decay and after the phase of symmetrical growth there is a phase with almost no friction. This result has been already obtained by Gualandris & Merritt (2008) and Read et al. (2006). In this regime, the star distribution is perturbed enough to change significantly the trajectory of the BH. To understand this phase, we can refer to equation (40). In Chandrasekhar's case, exchange of energy between the BH and a star happens only once. In our case, exchange is continuous and alternating. While at the beginning all stars coherently take energy from the BH, at this stage the coherence of energy exchange is lost owing to the dispersion of Ω_1 and the net energy transfer becomes zero (equation 39).

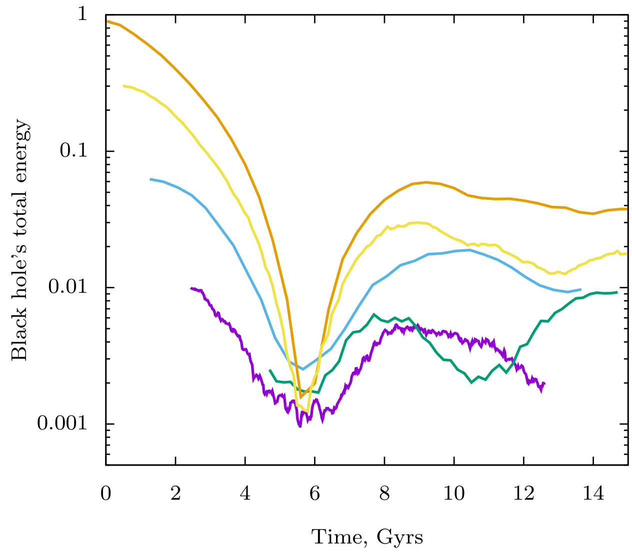

Figure 14. Dependence of the third-phase energy on the initial energy of the BH. $M = 10^{-3}M_g$, $m_{star} = 10^{-6}M_g$. Time is shifted according to equation (54), so that Brownian energy is reached at the same time for all energies.

Analysing the energy exchange between the massive satellite and stars at the stage of zero net energy change, Inoue (2011) pointed out that at this stage near-Chandrasekhar friction due to non-resonant particles is completely compensated by positive feedback from resonant particles, which constitute a very small fraction about 10^{-4} of all stars. From our point of view, this exact cancellation reveals the fact that 'resonant' and 'non-resonant' stars in terms of S. Inoue may be the same stars but at different phases of their permanent resonant interaction with the massive satellite. Indeed, as we see from equation (35) in permanent resonance periods of positive and negative energy transfer form a star to the BH alternate according to the sine law. So for an individual star periods of quick energy transfer change to periods of slow energy transfer, while the average energy flux form all stars at this stage remains at zero.

4.5 Final energy decay

The results of Gualandris & Merritt (2008) and Read et al. (2006) demonstrate slow energy decay at the final stage of satellite motion. This residual friction can be explained as Chandrasekhar's friction caused only by non-resonant stars. However, our model fails to describe the final energy decay of the BH. The perturbation of the star field caused by the BH never vanishes in our model because we have neglected pair encounters of the stars. This interaction leads to the star field relaxation in the second order of perturbation theory. This means that it is of the order of $M/M_g = 10^{-3}$. Thus our model fails to describe the galaxy after $\omega T \approx 10^3$.

4.6 Conclusions

We have investigated the motion of a massive perturber in a purely constant-density sphere analytically and numerically. This model can be considered as an idealization of real constant density cores, and has the advantage of relative analytical simplicity. This model captures the main property of constant-density cores underlying non-Chandrasekhar dynamical friction effects the full resonance of the perturber with all the stars in a harmonic potential. We have shown that when inside the core the perturber first experience a short stage of enhanced super-Chandrasekhar friction, then a stage of temporal energy increase, and finally a stage with no average friction, when the perturber energy randomly fluctuates about some constant value. This stage is the last in our model, and we do not see relaxation to the regime of Brownian fluctuations, because we neglect the relaxation due to pair collisions of the BPs. We have observed qualitatively the same behaviour of the perturber energy evolution both for circular and radial orbits. We have obtained an analytical formula for the perturber energy decay rate at the stage of super-Chandrasekhar friction and have shown that the dynamical friction force at this stage is half an order in M_{object}/M_{core} stronger than in Chandrasekhar's case. Numerical calculation of the decay time at the super-Chandrasekhar stage on the perturber mass confirms our analytical relationship. Our analytical formula is also in a good agreement with *N*-body data of other authors.

ACKNOWLEDGEMENT

The authors thank K. Zybin and E. Vasiliev for valuable discussion of the results.

REFERENCES

Antonini F., Merritt D., 2011, ApJ, 745, 83
Bate R., Mueller D., White J., 1971, Fundamentals of Astrodynamics. Dover Publications, Inc, NY
Binney J. J., Evans N. W., 2001, MNRAS, 327, L27
Binney J., Tremaine S., 1950, Galactic Dynamics. Princeton Univ. Press, Princeton
Bontekoe T. R., van Albada T. S., 1987, MNRAS, 323, 285
Borrielli A., Salucci P., 2001, MNRAS, 323, 285
Campanelli M., Lousto C., Zlochower Y., Merritt D., 2007, ApJ, 659, L5
Chandrasekhar S., 1943, ApJ, 97, 255
Colpi M., 1998, ApJ, 502, 167 (C98)
Colpi M., Pallavicini A., 1998, ApJ, 525, 720
Cora S. A., Muzzio J. C., Vergne M. M., 1997, MNRAS, 289, 253
de Blok W. J. G., McGaugh S. S., Bosma A., Rubin V. C., 2001, ApJ, 552, L23
Goerdt T., Moore B., Read J. I., Stadel J, Zemp M., 2006, MNRAS 368, 1073
Goerdt T., Moore B., Read J. I., Stadel J., 2010, ApJ, 725, 1707
González J. A., Hannam M., Sperhake U., Brügmann B., Husa S., 2007, Phys. Rev. Lett., 98, 231101
Gualandris A., Merritt D., 2008, ApJ, 678, L780
Inoue S., 2011, MNRAS, 416, 1181
Kalnajs A. J., 1972, ApJ, 175, 63
Kleyna J. T., Wilkinson M. I., Gilmore G., Evans N. W., 2003, ApJ, 588, L21
Lezhnin K. V., Chernyagin S. A., 2014, Astron. Lett., 40, 382
Lynden-Bell D., Kalnajs A. J., 1972, MNRAS 157, 1
Mulder W. A., 1983, A&A, 117, 9
Peñarrubia J., Just A., Kroupa P., 2004, MNRAS, 349, 747
Read J. I., Goerdt T., Moore B., Pontzen A. P., Stadel J., Lae G., 2006, MNRAS, 373, 1451
Tichy W., Marronetti P., 2007, Phys. Rev. D, 76, 061502
Tremaine S., Weinberg M. D., 1984, MNRAS, 209, 729
Weinberg M. D., 1986, ApJ, 300, 93
White S. D. M., 1976, MNRAS, 174, 467
White S. D. M., 1983, ApJ, 274, 53
Zaritsky D., White S. D. M., 1988, MNRAS, 235, 289

APPENDIX A: METHOD APPLICATION TO DERIVE CHANDRASEKHAR'S FORMULA

As an illustration of the method developed in this article let's derive the dynamical friction on the BH with mass M moving with constant velocity $\boldsymbol{V}$ through an infinite homogeneous field of stars. Hereinafter, we denote the position, velocity, momentum and mass of a single star by $\boldsymbol{r}$, $\boldsymbol{v}$, $\boldsymbol{p}$ and m, and the corresponding properties of the BH by $\boldsymbol{R}$, $\boldsymbol{V}$, $\boldsymbol{P}$ and M. Our goal is to reproduce the well-known Chandrasekhar's formula (1).

In order to use the perturbation theory we require the effect of the BH on every star to be treated as a small perturbation. First we try to find the trajectory of a single star, influenced by the BH. Without perturbation Hamilton equations for a single star are:

$$\dot{\boldsymbol{r}} = \frac{\partial H}{\partial \boldsymbol{p}}; \quad \dot{\boldsymbol{p}} = -\frac{\partial H}{\partial \boldsymbol{r}}, \tag{A1}$$

where $\boldsymbol{r} = \boldsymbol{r}(\boldsymbol{r}_0, \boldsymbol{p}_0, t)$, $\boldsymbol{p} = \boldsymbol{p}(\boldsymbol{r}_0, \boldsymbol{p}_0, t)$, H is the Hamiltonian of the system, $\boldsymbol{r}_0$, $\boldsymbol{p}_0$ are initial values of the phase variables.

After introducing a perturbation V the Hamiltonian becomes $H_1 = H + V$, and the initial data can be considered as functions of time: $\boldsymbol{r}_0 = \boldsymbol{r}_0(\boldsymbol{c}_1, \boldsymbol{c}_2, t)$, $\boldsymbol{p}_0 = \boldsymbol{p}_0(\boldsymbol{c}_1, \boldsymbol{c}_2, t)$. Then from Hamilton equations for H_1 and equation (A1) we get:

$$\frac{\partial \boldsymbol{r}}{\partial \boldsymbol{r}_0}\frac{\mathrm{d}\boldsymbol{r}_0}{\mathrm{d}\boldsymbol{t}} + \frac{\partial \boldsymbol{r}}{\partial \boldsymbol{p}_0}\frac{\mathrm{d}\boldsymbol{p}_0}{\mathrm{d}\boldsymbol{t}} = \frac{\partial V}{\partial \boldsymbol{p}} \tag{A2}$$

and

$$\frac{\partial \boldsymbol{p}}{\partial \boldsymbol{r}_0}\frac{\mathrm{d}\boldsymbol{r}_0}{\mathrm{d}\boldsymbol{t}} + \frac{\partial \boldsymbol{p}}{\partial \boldsymbol{p}_0}\frac{\mathrm{d}\boldsymbol{p}_0}{\mathrm{d}\boldsymbol{t}} = -\frac{\partial V}{\partial \boldsymbol{r}}. \tag{A3}$$

In Chandrasekhar's case unperturbed Hamiltonian is simply

$$H = \frac{p^2}{2m}, \tag{A4}$$

and the perturbation due to the BH in Newtonian limit is

$$V = -GmM/|\boldsymbol{r} - \boldsymbol{R}|. \tag{A5}$$

Unperturbed trajectories of the stars and of the BH are

$$\begin{aligned} \boldsymbol{r} &= \boldsymbol{r}_0 + \frac{\boldsymbol{p}_0}{m}t \\ \boldsymbol{p} &= \boldsymbol{p}_0, \end{aligned} \tag{A6}$$

and

$$\begin{aligned} \boldsymbol{R} &= \boldsymbol{R}_0 + \frac{\boldsymbol{P}_0}{M}t \\ \boldsymbol{P} &= \boldsymbol{P}_0, \end{aligned} \tag{A7}$$

Putting equation (A6) into equations (A2) and (A3) and taking into account equations (A5) and (A7), we obtain the following equations

$$\begin{aligned} &\dot{\boldsymbol{r}}_0 + \frac{t}{m}\dot{\boldsymbol{p}}_0 = 0 \\ &\dot{\boldsymbol{p}}_0 = GMm\frac{\partial}{\partial \boldsymbol{r}}\frac{1}{|\boldsymbol{r} - \boldsymbol{R}|} \end{aligned} \tag{A8}$$

which can be rewritten in the form

$$\begin{aligned} \dot{\boldsymbol{a}} &= GM\frac{\partial}{\partial \boldsymbol{b}}\frac{1}{|\boldsymbol{a} + \boldsymbol{b}t|} \\ \dot{\boldsymbol{b}} &= -GM\frac{\partial}{\partial \boldsymbol{a}}\frac{1}{|\boldsymbol{a} + \boldsymbol{b}t|}, \end{aligned} \tag{A9}$$

where

$$\begin{aligned} \boldsymbol{a} &= \boldsymbol{r}_0 - \boldsymbol{R}_0 \\ \boldsymbol{b} &= \frac{\boldsymbol{p}_0}{m} - \frac{\boldsymbol{P}_0}{M} \end{aligned} \tag{A10}$$

are the position and the velocity of the star in the BH reference frame, respectively. From equation (A9), it can easily be derived that the angular momentum of the star in this frame

$$\boldsymbol{L} = [\boldsymbol{a} \times \boldsymbol{b}] \tag{A11}$$

is constant. Equations (A9) are the Hamilton equations with the Hamiltonian $GM|\boldsymbol{a} + \boldsymbol{b}t|^{-1}$. Let us consider the motion of the star averaged by a large period of time $2T$. Averaged Hamiltonian is now

$$I(\boldsymbol{a}, \boldsymbol{b}) = \frac{GM}{2T}\int_{-T}^{T}\frac{\mathrm{d}t}{|\boldsymbol{a} + \boldsymbol{b}t|} = \frac{GM}{2T|\boldsymbol{b}|}\ln\frac{4b^4T^2}{[\boldsymbol{a} \times \boldsymbol{b}]^2}. \tag{A12}$$

Below we assume that $T \to \infty$. As a result of averaging we get a classical Hamiltonian system for averaged values:

$$\dot{\boldsymbol{a}} = \frac{\partial I}{\partial \boldsymbol{b}}; \quad \dot{\boldsymbol{b}} = -\frac{\partial I}{\partial \boldsymbol{a}}. \tag{A13}$$

From equations (A9) and (A12) it follows that

$$\dot{\boldsymbol{b}} = -\frac{GM}{T}\frac{[\boldsymbol{b} \times \boldsymbol{L}]}{|\boldsymbol{b}|\boldsymbol{L}^2}. \tag{A14}$$

Multiplying this equation by $\boldsymbol{b}$ leads to $\dot{\boldsymbol{b}}^2 = 0$ and $|\boldsymbol{b}| = \text{const}$. Therefore, this is a simple rotational equation

$$\dot{\boldsymbol{b}} = [\boldsymbol{\Omega} \times \boldsymbol{b}] \tag{A15}$$

and

$$\boldsymbol{\Omega} = \frac{GM}{T}\frac{\boldsymbol{L}}{|\boldsymbol{b}|\boldsymbol{L}^2} = \text{const}. \tag{A16}$$

We see that averaging equation (A12) means the replacement of real star trajectories by segments of circles with the same net rotation angle.

The axis of rotation is $\boldsymbol{n} = \boldsymbol{L}/|\boldsymbol{L}|$ and the complete angle of rotation is

$$\theta = 2T\Omega = \frac{2GM}{|\boldsymbol{b}||\boldsymbol{L}|}. \tag{A17}$$

The solution is

$$\boldsymbol{b}_{\text{final}} = \mathbf{O}(\theta)\boldsymbol{b}_0, \tag{A18}$$

where $\mathbf{O}(\theta)$ is the matrix of rotation for an angle θ around the vector $\boldsymbol{n} = (x, y, z)$:

$$\begin{vmatrix} c + (1-c)x^2 & -sz + (1-c)xy & sy + (1-c)xz \\ sz + (1-c)xy & c + (1-c)y^2 & -sx + (1-c)yz \\ -sy + (1-c)xz & sx + (1-c)yz & c + (1-c)z^2 \end{vmatrix} \tag{A19}$$

where $c = \cos\theta$, $s = \sin\theta$. For the final star velocity we have

$$\boldsymbol{v}_{\text{final}} = \boldsymbol{V}_0 + \mathbf{O}(t)(\boldsymbol{v}_0 - \boldsymbol{V}_0). \tag{A20}$$

The star gains energy

$$\Delta E = \frac{m}{2}\left(\boldsymbol{v}_{\text{final}}^2 - \boldsymbol{v}_0^2\right) = m\left(\boldsymbol{V}_0 \cdot (\mathbf{O}(\theta) - \mathbf{1})(\boldsymbol{v}_0 - \boldsymbol{V}_0)\right), \tag{A21}$$

which can be rewritten in the form

$$\begin{aligned} \Delta E/m &= \sin\theta\frac{(\boldsymbol{V}_0 \cdot [\boldsymbol{L} \times (\boldsymbol{v}_0 - \boldsymbol{V}_0)])}{|\boldsymbol{L}|} \\ &\quad + (1 - \cos\theta)((\boldsymbol{v}_0 - \boldsymbol{V}_0) \cdot \boldsymbol{V}_0). \end{aligned} \tag{A22}$$

As the star field is infinite and homogeneous, the result cannot depend on the initial position of the BH. Therefore, we can take $\boldsymbol{R}_0 = 0$, and therefore $\boldsymbol{L} = [\boldsymbol{r}_0 \times (\boldsymbol{v}_0 - \boldsymbol{V}_0)]$. θ does not depend on the sign of $\boldsymbol{r}_0$ and thus after averaging on $\boldsymbol{r}_0$ the first component vanishes, and we get

$$\Delta E = m(1 - \cos\theta)((\boldsymbol{v}_0 - \boldsymbol{V}_0) \cdot \boldsymbol{V}_0). \tag{A23}$$

As we assume the influence of the BH on stars to be small, we take $\theta < <1$, and therefore cosine can be expanded into series, and

$$\Delta E = \frac{2G^2 M^2 m}{\boldsymbol{b}^2 \boldsymbol{L}^2}((\boldsymbol{v}_0 - \boldsymbol{V}_0) \cdot \boldsymbol{V}_0) \tag{A24}$$

or

$$\Delta E = \frac{2G^2 M^2 m}{\boldsymbol{r}_0^2 \sin^2\varphi} \frac{((\boldsymbol{v}_0 - \boldsymbol{V}_0) \cdot \boldsymbol{V}_0)}{|\boldsymbol{v}_0 - \boldsymbol{V}_0|^4}, \tag{A25}$$

where φ is the angle between $\boldsymbol{r}_0$ and $\boldsymbol{v}_0 - \boldsymbol{V}_0$.

Replacing m with $\rho \mathrm{d}^3\boldsymbol{r}_0$, integrating over all stars and defining the friction force as

$$F = \frac{\sum \Delta E}{2TV_0} = \frac{\sum \Delta E}{D} \tag{A26}$$

we get

$$F = 4\pi G^2 M^2 \rho D^{-1} \int_0^{D/2} \int_{\varphi_0}^{\pi-\varphi_0} \frac{r^2 \sin\varphi \mathrm{d}\varphi \mathrm{d}r}{r^2 \sin^2\varphi} \cdot \int_{\boldsymbol{v}_0} \frac{((\boldsymbol{v}_0 - \boldsymbol{V}_0) \cdot \boldsymbol{V}_0)}{|\boldsymbol{v}_0 - \boldsymbol{V}_0|^4} f(v_0) \mathrm{d}^3\boldsymbol{v}_0, \tag{A27}$$

where D is the size of the system, $f(v_0)$ is the velocity distribution assumed to be isotropic and $\varphi = \arcsin d/r$. d is the minimal distance between stars and the BH's trajectory. If we approximate the first integral assuming $d \ll D$, we have

$$F = 4\pi G^2 M^2 \rho \ln\frac{D}{d} \int_{\boldsymbol{v}_0} \frac{(\boldsymbol{v}_0 - \boldsymbol{V}_0 \cdot \boldsymbol{V}_0)}{|\boldsymbol{v}_0 - \boldsymbol{V}_0|^4} f(v_0) \mathrm{d}^3\boldsymbol{v}_0. \tag{A28}$$

The second integral depends much on $f(v)$, but if $v_0 \ll V_0$ it equals approximately V_0^{-2} and if $v_0 \gg V_0$ it tends to zero because of the symmetry. That is why

$$F = \frac{4\pi G^2 M^2}{V_0^2} \rho(<V_0) \ln\frac{D}{d}, \tag{A29}$$

which is identical to equation (1).

Logarithmic divergence of the integral at $|\boldsymbol{v}_0 - \boldsymbol{V}_0| = 0$ physically means that the large part of dynamical friction is exerted by stars with $\boldsymbol{v} \approx \boldsymbol{V}$, i.e. the stars moving in a 'resonance' with the BH. This result corresponds in some way with the result of Tremaine & Weinberg (1984), who revealed the importance of resonances for dynamical friction in spherical galaxies.

This paper has been typeset from a TeX/LaTeX file prepared by the author.